are in qualitative agreement with the calculations of Loudon, and Howard and Hasegawa. For a sample glued to a glass substrate the strain is relatively large and the magneto-absorption spectrum becomes rather complicated. An example of this can be seen from the measurements of ZLRB where at 77°K at least three zero field absorptions are observed.

A definitive experiment that would verify that the intense absorptions were due to excitons would be to measure the photoconductivity at $h\nu = E_{x_i}(B \neq 0)$. For a true exciton no photoconductive effect should appear. While this should in principle verify that the absorption is due to an exciton, it may be a difficult measurement to make because of effects such as impact ionization.

ACKNOWLEDGMENTS

The authors wish to acknowledge the Dr. F. Blatt, Dr. R. R. Goodman, and Dr. G. Weinreich for their helpful discussions and advice. Dr. R. W. Terhune Dr. C. W. Peters, and P. D. Maker for their assistance with the instrumentation. Dr. G. Weinreich of the Bell Telephone Laboratories, R. Petritz of the Texas Instruments Company, and W. C. Dunlap of Raytheon for supplying us with the intrinsic germanium crystals.

PHYSICAL REVIEW VOLUME 120, NUMBER 2 OCTOBER 15, 1960

Low-Temperature Specific Heat of Body-Centered Cubic Alloys of 3*d* Transition Elements*

C. H. CHENG, C. T. WEI, AND P. A. BECK
Department of Mining and Metallurgical Engineering, University of Illinois, Urbana, Illinois
(Received May 20, 1960)

The electronic specific heat coefficient was measured in the temperature range 1.4° to 4.2°K for 48 solid solution alloys in the following binary systems: Ti-V, V-Cr, V-Fe, Cr-Mn, Cr-Fe, and Fe-Co. The electronic specific heat vs electron concentration curves show three quite well separated regions of high density of states. The first of these occurs in alloys with atomic magnetic moments near zero. The second one is found in alloys which have increasing magnetic moments with increasing electron concentration, up to Fe+35% Co along the Pauling-Slater curve. The third region of high density of states extends from Fe+35% Co to the limit of the bcc solid solutions at Fe+75% Co, a range where the magnetic moment decreases with increasing electron concentration.

INTRODUCTION

THE details of the structure of the *d* band for 3*d* transition elements in the solid state are not definitely known as yet. Various points of view were recently discussed by Mott and Stevens,[1] Lomer and Marshall,[2] and Marshall and Weiss.[3] Experimentally, measurement of the electronic specific heat at low temperatures gives information on the density of states at the Fermi energy level. In the 3*d* transition elements and their alloys the major contribution to the density of states comes from the *d* band. By measuring the electronic specific heat for a series of isostructural solid solution alloys, the density of states in the *d* band can be determined as a function of the electron concentration (the average number of electrons per atom outside the closed argon shell). Low-temperature specific heat results for body-centered cubic Cr-Fe and Cr-Mn alloys have been already published in a brief note.[4] The coefficient of the term of the low-temperature specific heat linear in temperature was found to reach very high values in alloys near Cr+19 at. % Fe, and in the corresponding Cr-Mn alloys. At the time this note was published, it was uncertain whether or not these very high values might be interpreted as electronic specific heat coefficients. The present paper reviews recent information bearing on this question, and it provides additional data extending the electron concentration range of the bcc alloys studied. Measurements were made with 48 alloys in the binary systems Ti-V, V-Cr, Cr-Fe, Fe-Co, V-Fe, and Cr-Mn.

EXPERIMENTAL PROCEDURES

Most of the alloys were prepared by induction melting in recrystallized alumina crucibles in He of one atmosphere. Alloys containing vanadium were arc melted in a water-cooled copper crucible under He atmosphere. All alloy specimens were homogenized for three days at 1170°C in a purified mixture of 92% He+8% H_2 gas, wrapped in Mo or Nb sheets. At the end of the homogenizing anneal the specimens were quenched in cold water. After this treatment, some alloy specimens were cold worked and reannealed at the following temperatures: The $Cr_{0.06}Fe_{0.94}$ specimen

* This work was supported by the U. S. Air Force, Wright Air Development Center.
[1] N. F. Mott and K. W. H. Stevens, Phil. Mag. **2**, 1364 (1957).
[2] W. M. Lomer and W. Marshall, Phil. Mag. **3**, 185 (1958).
[3] W. Marshall and R. J. Weiss, Suppl. J. Appl. Phys. **30**, 220S (1959).
[4] C. T. Wei, C. H. Cheng, and P. A. Beck, Phys. Rev. Letters **2**, 95 (1959).

TABLE I. Chemical, spectrographic, and gas analysis of specimens.[a]

Nominal composition	Analysis wt % V	Ti	Mn	Fe	Co	Al	Si	Cu	W	O_2	H_2	N_2	Calculated at. % ratio V	Ti	Mn	Fe
$Ti_{0.5}V_{0.5}$	52.64	47.31						0.0X		0.0730	0.103	0.0359	51.13	48.87		
		Cr												Cr		
$V_{0.77}Cr_{0.23}$	76.42	23.10								0.798	0.0026	0.279	77.16	22.84		
$V_{0.5}Cr_{0.5}$	49.57	50.38		0.00X		N.D.	0.00X		0.000X				50.11	49.89		
	48.28	51.26											49.02	50.98		
$V_{0.26}Cr_{0.74}$	25.47	74.01								0.340	0.0011	0.0192	26.00	74.00		
	25.60	74.12											26.07	73.93		
$V_{0.2}Cr_{0.8}$	19.80	80.14			0.01			0.01		0.406	0.0006	0.0402	20.14	79.86		
$V_{0.1}Cr_{0.9}$	10.11	89.82			0.01			N.D.		0.439	0.0006	0.0024	10.30	89.70		
$V_{0.05}Cr_{0.95}$	5.05	94.92			0.01			0.03		0.430	0.0006	0.0122	5.15	94.85		
$Cr_{0.9}Mn_{0.1}$		89.24	10.72	0.00X		0.0X	0.0X		N.D.					89.79	*t* 10.21	
		90.13	9.85											90.62	*b* 9.38	
$Cr_{0.8}Mn_{0.2}$		78.68	21.25	0.00X		0.00X	0.00X		N.D.					79.63	*t* 20.37	
		80.51	19.48											81.36	*b* 18.64	
$Cr_{0.69}Mn_{0.31}$		68.45	31.49	0.00X		0.00X	0.00X		N.D.					69.66	*t* 30.34	
		67.58	32.41											68.77	*b* 31.23	
$Cr_{0.61}Mn_{0.39}$		60.37	39.60			0.0035	0.0005			0.431	0.012			61.69	*t* 38.31	
		58.80	41.15											60.15	*b* 39.85	
$Cr_{0.5}Mn_{0.5}$		47.89	51.92			0.0X	0.0X	0.0X		0.179	0.0016	0.0247		49.35	50.65	

Nominal composition	Analysis wt % V	Cr	Mn	Fe	Co	Al	Si	Cu	W	O_2	H_2	N_2	Calculated at. % ratio V	Fe
$V_{0.92}Fe_{0.08}$	91.19			8.79				N.D.	N.D.	0.537	0.0099	0.554	91.92	8.08
$V_{0.85}Fe_{0.15}$	83.73			16.19				N.D.	N.D.	0.123	0.0029	0.0905	85.00	15.00
$V_{0.8}Fe_{0.2}$	77.97			21.93				N.D.	N.D.	0.162	N.D.	0.0507	79.58	20.42
$V_{0.76}Fe_{0.24}$	73.78			25.80						0.247	0.0041	0.243	75.81	24.19
$V_{0.74}Fe_{0.26}$	72.55			27.40				N.D.	N.D.				74.37	25.63
$V_{0.72}Fe_{0.28}$	70.51			29.45				N.D.	N.D.	0.177	0.0017	0.359	72.41	27.59
$V_{0.7}Fe_{0.3}$	67.11			32.88				N.D.	N.D.	0.135	0.0005	0.0803	69.11	30.89
$V_{0.69}Fe_{0.31}$			0.0X		0.0X		0.0X			0.113	0.0014	0.0539		
$V_{0.66}Fe_{0.34}$	64.01	0.00X		35.97		0.00X	0.00X		N.D.				66.11	33.89
	63.29			36.69									65.41	34.59
$V_{0.55}Fe_{0.45}$	52.55			47.40				N.D.	N.D.	0.280	0.0006	0.0504	54.86	45.14
$V_{0.33}Fe_{0.67}$	31.36			68.60				N.D.	N.D.	0.0594	0.0013	0.0516	33.38	66.62
									Ni				Cr	
$Cr_{0.98}Fe_{0.02}$		97.35		2.12		0.X	0.00X	0.0000		0.3460	0.0004	0.0021	98.0	2.0
$Cr_{0.95}Fe_{0.05}$		94.54	0.00X	4.97		0.00X	0.0X			0.389	0.0005	0.00141	95.3	4.7
$Cr_{0.90}Fe_{0.10}$		88.87	0.00X	10.56		0.00X	0.0X			0.2860	0.0004	0.0108	90.0	10.0
$Cr_{0.84}Fe_{0.16}$		82.88	0.00X	17.05		0.00X	0.0X			0.3970	0.0004	0.0079	83.9	16.1
$Cr_{0.82}Fe_{0.18}$		80.64	0.0X	19.27		0.00X	0.0X			0.3390	0.0010	0.0130	81.8	18.2
$Cr_{0.81}Fe_{0.19}$		79.32	0.00X	20.48	N.D.	0.00X	0.00X	N.D.	N.D.	0.1370	0.0009	0.2630	80.6	19.4
$Cr_{0.80}Fe_{0.20}$		78.48		21.50		0.0003	0.009			0.332	0.001	0.0016	79.7	*t* 20.3
		78.43		21.51		0.0005	0.009			0.408	0.001		79.7	*b* 20.3
$Cr_{0.70}Fe_{0.30}$		68.52		31.16	N.D.	N.D.	N.D.	0.00X	N.D.	0.2640	0.0011	0.0027	70.3	29.7
$Cr_{0.63}Fe_{0.37}$		60.77		39.20		0.0005	0.009			0.2370	0.0006	0.0018	62.5	*t* 37.5
		61.05		38.93		0.0004	0.009						62.7	*b* 37.3
$Cr_{0.53}Fe_{0.47}$		51.50	0.X	48.18	N.D.	0.00X	0.00X	0.0000X	N.D.	0.0914	0.0001	0.0072	53.4	46.6
$Cr_{0.22}Fe_{0.78}$		21.14		78.65		0.0006	0.18			0.0598	0.0001	0.0072	22.4	*t* 77.6
		21.12		78.66		0.0004	0.16			0.088	0.00014		22.4	*b* 77.6
$Cr_{0.15}Fe_{0.85}$		14.01		85.94		N.D.	0.00X			0.0625	0.0003	0.0001	14.9	85.1
$Cr_{0.06}Fe_{0.94}$		5.32	0.0X	94.58	N.D.	N.D.	0.00X	N.D.	N.D.	0.0384	$<10^{-6}$	0.0007	5.7	94.3
Fe		N.D.		99.96	N.D.	0.0X		N.D.	N.D.	0.0012	$<5\times10^{-7}$	0.0002		100

Nominal composition	Analysis wt % Cr	Mn	Fe	Co	Al	Si	Cu	Ni	O_2	H_2	N_2	Calculated at. % ratio Co	Fe
$Fe_{0.90}Co_{0.10}$	0.0X		89.94	9.90	0.0X		0.0X	N.D.	0.0064	6×10^{-7}	0.0002	9.5	90.5
$Fe_{0.86}Co_{0.14}$	N.D.		84.82	15.10	0.00X		0.0X	0.0X	0.0034	8×10^{-7}	0.0002	14.4	85.6
$Fe_{0.76}Co_{0.24}$	N.D.		74.88	24.96	0.00X		0.X	0.X	0.0100	1.3×10^{-6}	0.0002	24.0	76.0
$Fe_{0.70}Co_{0.30}$	0.0000X	0.0X	68.37	31.32	0.00X	0.00X	0.000X	0.X	0.0044	$<5\times10^{-7}$	0.0001	30.3	69.7
$Fe_{0.66}Co_{0.34}$	N.D.		64.22	35.24	0.00X		0.X	0.X	0.0053	8×10^{-7}	0.0009	34.2	65.8
$Fe_{0.62}Co_{0.38}$	N.D.		61.06	38.70	0.0X		0.X	0.X	0.0118	2.5×10^{-6}	0.0008	37.5	62.5
$Fe_{0.49}Co_{0.51}$	N.D.		47.60	52.20	0.00X		0.X	0.X	0.0149	8.1×10^{-6}	0.0009	51.0	49.0
$Fe_{0.40}Co_{0.60}$	N.D.		38.95	60.85	0.00X		0.X	0.X	0.0035	1.4×10^{-6}	0.0002	59.7	40.3
$Fe_{0.31}Co_{0.69}$	0.0000X	N.D.	29.53	69.04	0.00X	0.00X	0.000X	0.X	0.0049	$<5\times10^{-7}$	0.0002	68.9	31.1
$Fe_{0.28}Co_{0.72}$	N.D.		26.61	73.05	0.00X		0.X	0.X	0.0025	1.5×10^{-6}	0.0001	72.2	27.8
$Fe_{0.25}Co_{0.75}$			24.23	75.62			0.X	0.X	0.0100	$<10^{-6}$	0.0002	74.7	25.3
$Fe_{0.07}Co_{0.93}$	N.D.		6.91	92.75	0.00X		0.X	0.X	0.0026	7×10^{-7}	0.0001	92.7	7.3
Co	N.D.		0.X	99.56	0.0X		0.X	0.X	0.0026	$<5\times10^{-7}$	0.0001	100	

[a] N.D.—Not detected; *t*—top; *b*—bottom; *X*—an undetermined nonzero digit.

was reannealed for two days at 800°C, $Fe_{0.75}Co_{0.25}$ was reannealed for two days at 650°C, $Fe_{0.5}Co_{0.5}$, and $Fe_{0.07}Co_{0.93}$ were not reannealed, and all other Fe-Co alloys were reannealed for two days at 800°C after cold working. The induction-melted ingots were cut into two disks. Of each arc-melted alloy two buttons were prepared, with as nearly identical composition as possible. Table I gives the nominal composition, chemical, spectroscopic, and gas analysis for each specimen. In many cases separate chemical analyses were made of the bottom and the top portions of induction melted ingots. As seen in Table I, these analyses agreed in all cases within less than 1%. The total weight of the two disks or the two buttons of each alloy, which were used together for the measurements, corresponded approximately to 1 mole. After the measurements made in the usual way were completed, the $Cr_{0.81}Fe_{0.19}$ alloy specimens were machined to a smaller size amounting to approximately 0.3 mole for use in the specific heat determination in magnetic field. The decrease in the size of this specimen was necessitated by the limited space between the poles of the magnet.

The calorimeter can with the specimen was cooled to about 1.2°K by lowering the pressure over the liquid He bath to about 1 mm Hg. After pumping out the exchange gas from the calorimeter can the measurements were carried out by introducing into the specimen known amounts of electrical energy in successive steps, and measuring accurately the temperature rise at each step. The calorimeter has been described previously.[5] A new feature in the present measurements was the use of a disk-shaped heater-thermometer assembly. This form has the advantage that it can be used for alloys which are too hard to be drilled and machined accurately. A $\frac{1}{10}$-watt carbon thermometer was fitted into the $\frac{1}{16}$-in. bore drilled parallel to the flat surfaces of the $\frac{3}{4}$-in. diameter and $\frac{1}{8}$-in. thick copper disk. The carbon thermometer was electrically insulated from, and thermally connected to, the copper block by means of glyptal. Approximately 9 feet of No. 40 B. & S. gage nylon-covered manganin wire was wound noninductively into the groove machined around the periphery of the copper disk. The wire heater had a resistance of approximately 300 ohms at 4.2°K, and a temperature coefficient of 0.0004/°K. A thin film of silicone grease was applied to that surface of each specimen, which was flat ground and polished in order to obtain good thermal

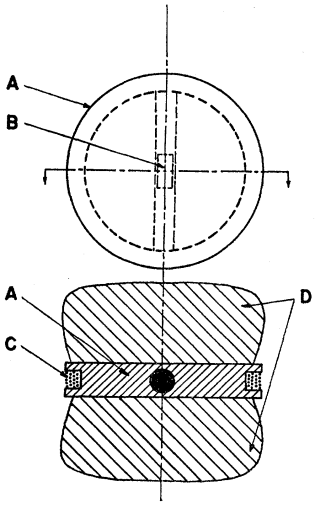

FIG. 1. Heater-thermometer assembly. A—copper disk; B—carbon thermometer; C—manganin heater; D—specimen.

[5] C. T. Wei, C. H. Cheng, and P. A. Beck, Phys. Rev. **112**, 696 (1958).

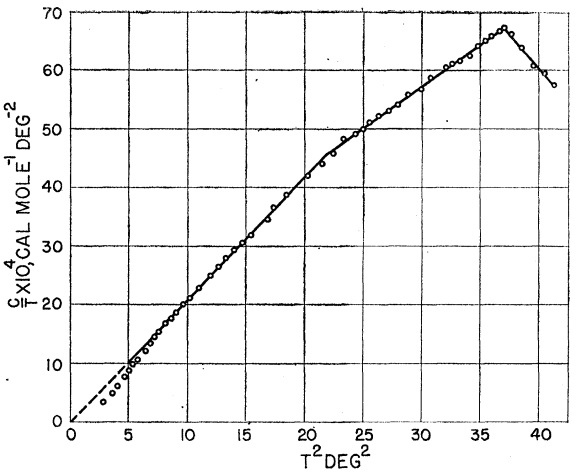

FIG. 2. Specific heat of $Ti_{0.5}V_{0.5}$ alloy. Superconducting transition temperature corresponds to peak at 6.09°K.

TABLE II. Specific heat of $V_{0.1}Cr_{0.9}$.

T °K	C 10^{-4} cal/ mole deg	C/T 10^{-4} cal/ mole deg^2	T^2 (°K)^2
1.407	7.29	5.180	1.98
1.428	7.54	5.283	2.04
1.450	7.57	5.223	2.10
1.474	7.70	5.224	2.17
1.500	7.94	5.290	2.25
1.532	8.10	5.286	2.35
1.570	8.32	5.297	2.47
1.618	8.57	5.300	2.62
1.673	8.87	5.302	2.80
1.739	9.20	5.291	3.02
1.824	9.67	5.301	3.33
1.935	10.3	5.315	3.74
2.020	10.8	5.334	4.08
2.106	11.2	5.341	4.43
2.226	11.9	5.341	4.95
2.385	12.8	5.376	5.69
2.523	13.6	5.371	6.37
2.640	14.3	5.425	6.97
2.795	15.2	5.434	7.81
2.994	16.5	5.526	8.96
3.138	17.4	5.548	9.85
3.236	18.0	5.550	10.5
3.352	18.7	5.582	11.2
3.489	19.6	5.631	12.2
3.636	20.6	5.665	13.2
3.772	21.6	5.736	14.2
3.848	22.0	5.730	14.8
3.952	22.7	5.742	15.6
4.073	23.6	5.799	16.6

contact with the polished faces of the heater-thermometer assembly sandwiched between two specimens, Fig. 1. The sandwich was held together tightly with No. 18 gage copper wire. The assembly was hung inside the calorimeter can by means of thin nylon thread.

The heating currents used successively in each experiment were 0.2, 0.3, 0.5, and 1.0 ma, with the heating time kept in the range of 10–60 seconds, and measured by means of a precision 1000-cps signal generator and an electronic counter. The current passing through the carbon thermometer was held at 1 μa during both calibration and measurement. In the case of the superconductive $Ti_{0.5}V_{0.5}$ alloy specimen, measurements were made up to 6.5°K, in order to reach the transition temperature. In this higher temperature range, where the resistance of the carbon thermometer was quite

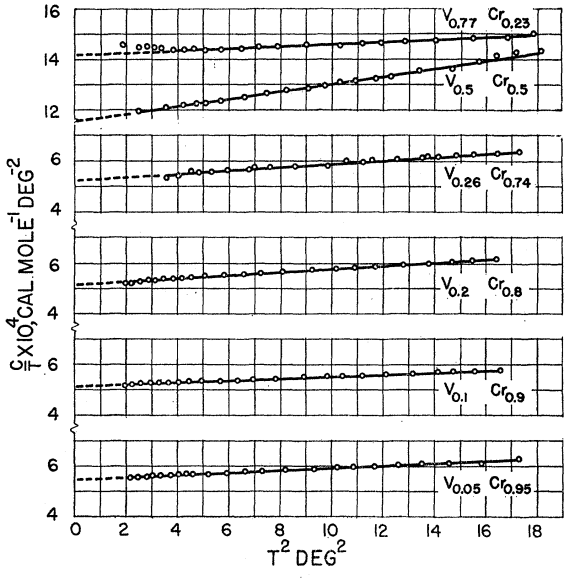

FIG. 3. Specific heat of bcc V-Cr solid solutions.

low, the current had to be increased to 10 μa. The voltage drop across the carbon thermometer was slightly overbalanced by an opposing emf from a K-3 potentiometer, and the difference was amplified by means of a dc microvolt amplifier, the output of which was fed into a high-speed millivolt recorder.

Measurements were normally made between 1.4° and 4.2°K, where the carbon thermometer could be directly calibrated against the He pressure, using the 1955 helium temperature scale,[6] T_{55E}. During calibration correction was made for the pressure of the column of liquid helium over the center line of the specimen. It was found that in the temperature range from 1.2° to 4.2°K the resistance of the carbon thermometers used could be fitted very accurately to the two-parameter equation $[(\log R)/T]^{\frac{1}{2}}=A+B\log R$. The parameters A

[6] J. R. Clement, J. K. Logan, and J. Gaffney, Phys. Rev. **100**, 743 (1955).

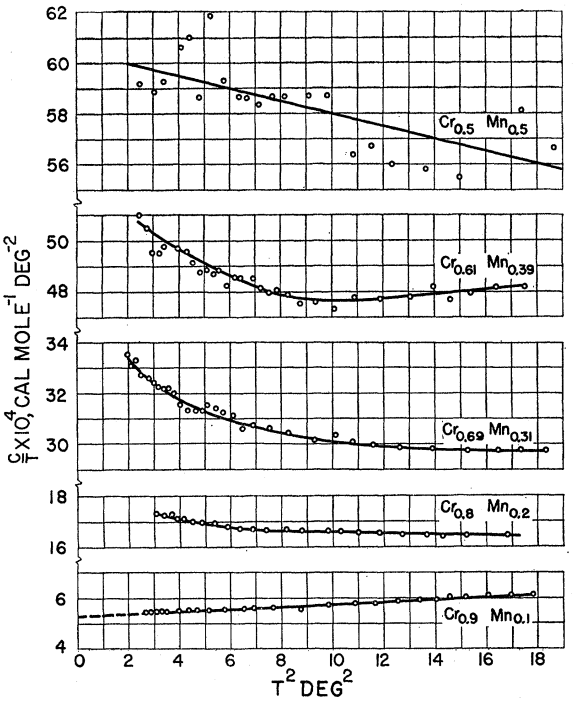

FIG. 4. Specific heat of bcc Cr-Mn solid solutions.

and B were very constant for each carbon thermometer over long periods of use. For different carbon thermometers the values of the parameters varied somewhat. A specific heat determination was made in a magnetic field of 1000 oe. The carbon thermometer calibrations made with and without the magnetic field did not differ from each other within the accuracy of the measurements. In the case of the superconductive alloy specimen $Ti_{0.5}V_{0.5}$, measurements were made from

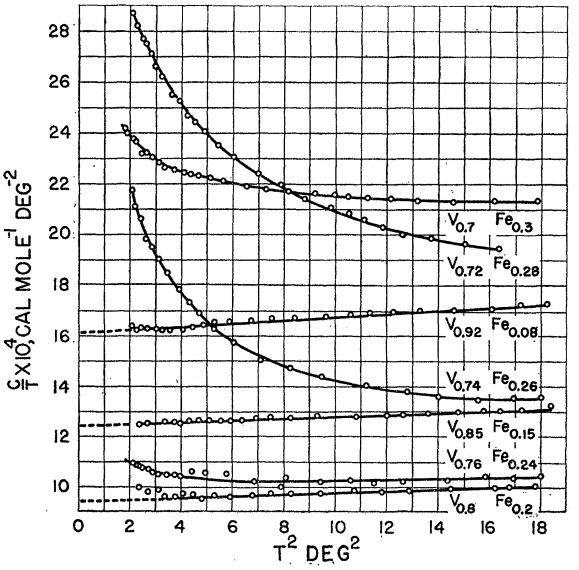

FIG. 5. Specific heat of bcc V-Fe solid solutions.

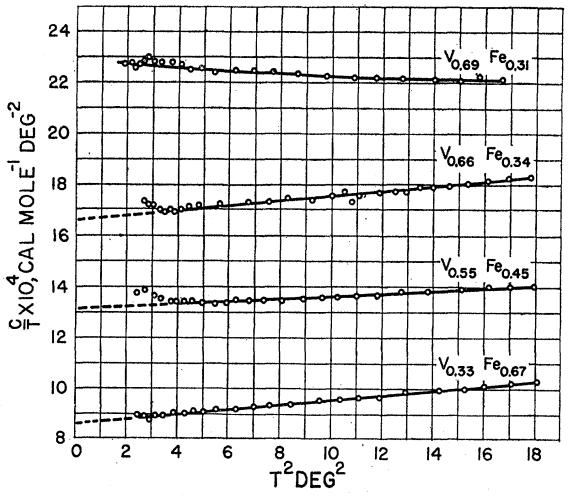

FIG. 6. Specific heat of bcc V-Fe solid solutions.

1.7° to 6.5°K, although above 4.2°K no calibration was available. The calibration, carried out below 4.2°K, was extrapolated by using the above equation.

All specimens were examined metallographically. The V-Fe alloys with high V content were found to have numerous fine cracks. Similar cracks were also found in the Cr-Mn alloys at high Mn contents. In the Cr-Mn alloys fine plate-like second-phase particles were found dispersed in the bcc matrix. These platelets were not present in the alloys in the as-melted condition, but were formed during the homogenizing anneal. It seems likely that these platelets are particles of a complex nitride phase, formed by the N_2 impurity in the reducing gas mixture in which the specimens were annealed. Small round oxide inclusions representing a very small volume fraction of the specimens were found in the Cr-Fe alloys. X-ray diffraction patterns were made of the homogenized specimens used for the specific heat measurements, in order to ascertain the crystal structure. Four Cr-Fe alloys were tested, including $Cr_{0.81}Fe_{0.19}$. All these alloys, and also $Cr_{0.5}Mn_{0.5}$ and $V_{0.25}Cr_{0.75}$, were found to be body-centered cubic. Of the four Fe-Co alloys tested three were bcc, including $Fe_{0.27}Co_{0.73}$, which was reannealed at 800°C. Alloy $Fe_{0.07}Co_{0.93}$, which was quenched from 1170°C, had face-centered cubic structure. The crystal structure of each alloy specimen is listed in Table III.

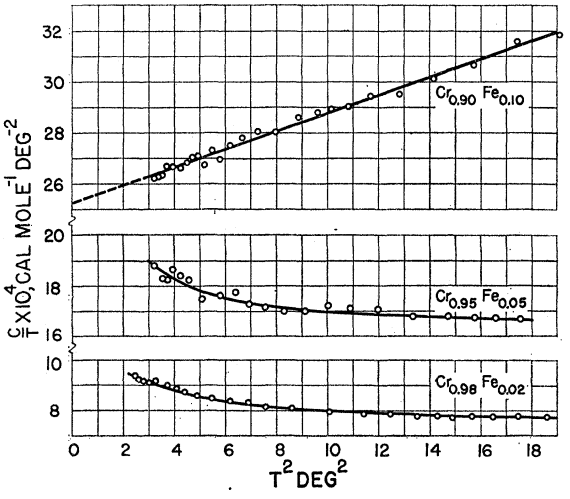

FIG. 7. Specific heat of bcc Cr-Fe solid solutions.

RESULTS

Typical data for an alloy ($V_{0.1}Cr_{0.9}$) is given in Table II.[7] Figs. 2 to 12 show the C/T vs T^2 plots for all alloys. The γ and θ values derived from the experimental data are listed in Table III. Alloy $Ti_{0.5}V_{0.5}$ is superconductive at low temperatures; the maximum of the C/T, Fig. 2, which corresponds to the superconducting transition temperature occurs at 6.09°K. This

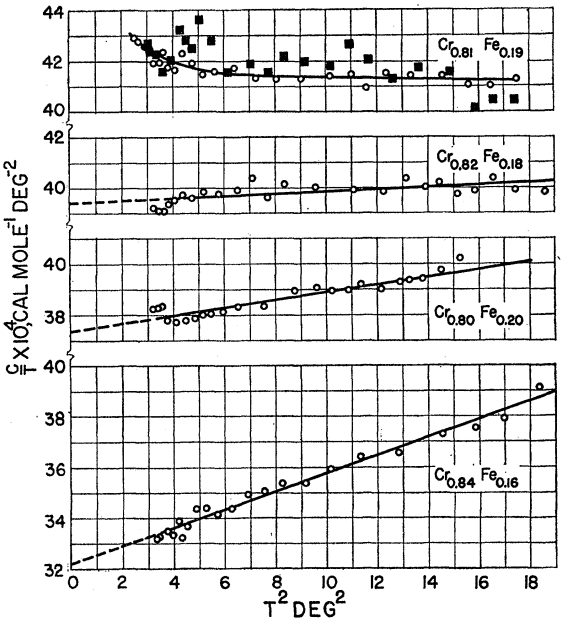

FIG. 8. Specific heat of bcc Cr-Fe solid solutions. (Filled squares represent specific heat measurements in a magnetic field of 1000 oe.)

is higher than the transition temperature of either component of the alloy. The change in slope at 4.77°K in the C/T vs T^2 line is similar to that previously found for V[8] and for Ta[9,10] in the superconductive state. At the lowest temperatures the measured specific heat values are distinctly lower than expected on the basis of the T^3 relationship for superconductors. The γ value

[7] All data obtained are available in tabular form on request from P. A. Beck, 205 Transportation Building, University of Illinois, Urbana, Illinois.

[8] W. S. Corak, B. B. Goodman, C. B. Satterthwaite, and A. Wexler, Phys. Rev. **96**, 1442 (1954).

[9] W. H. Keesom and M. Desirant, Physica **8**, 273 (1941).

[10] R. D. Worley, M. W. Zemansky, and H. A. Boorse, Phys. Rev. **91**, 1567 (1953).

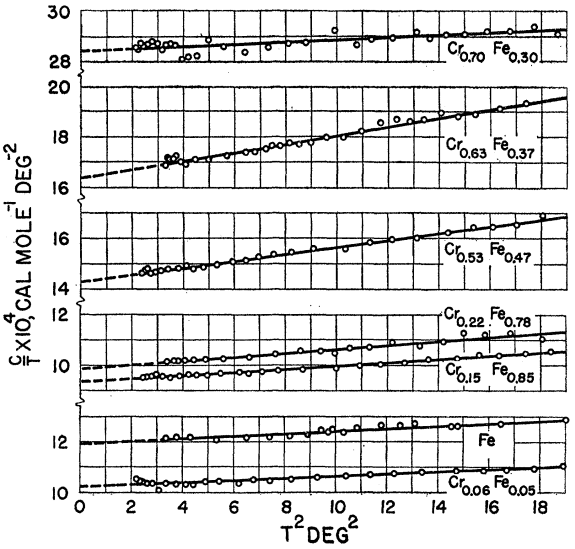

FIG. 9. Specific heat of bcc Cr-Fe solid solutions. *Note added in proof*. The composition indicated for the bottom curve is incorrectly specified. It should read "$CR_{0.06}Fe_{0.94}$."

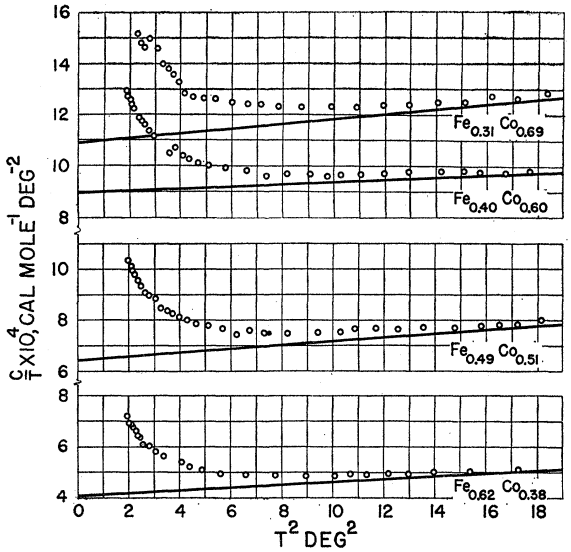

FIG. 11. Specific heat of bcc Fe-Co solid solutions. [Solid lines represent electronic plus lattice contribution, as calculated from Eq. (2).]

for the normal state of the alloy, given in Table III, was calculated by equating the entropy at the transition temperature for the normal and the superconducting states, as suggested by Corak *et al.*[8] For the purposes of this calculation θ for the alloy was assumed to be 385°K, obtained by averaging the Debye temperatures of Ti and V.

As seen in Fig. 3, the C/T vs T^2 plots for the V-Cr alloys are straight lines, conforming to the equation

$$C=\gamma T+\beta T^3. \qquad (1)$$

The coefficients γ and β, and the standard deviation ϵ of the data points from the least squares fit according to Eq. (1), are listed for each alloy in Table III. It is seen in Fig. 3 that for alloy $V_{0.77}Cr_{0.23}$ the lowest-temperature data points slightly deviate upward from the straight line extrapolated from the other data points. This deviation, which was found to occur in several other cases as well, is presumably caused by the re-evaporation of adsorbed He exchange gas from the surface of the specimen in the earliest stages of the

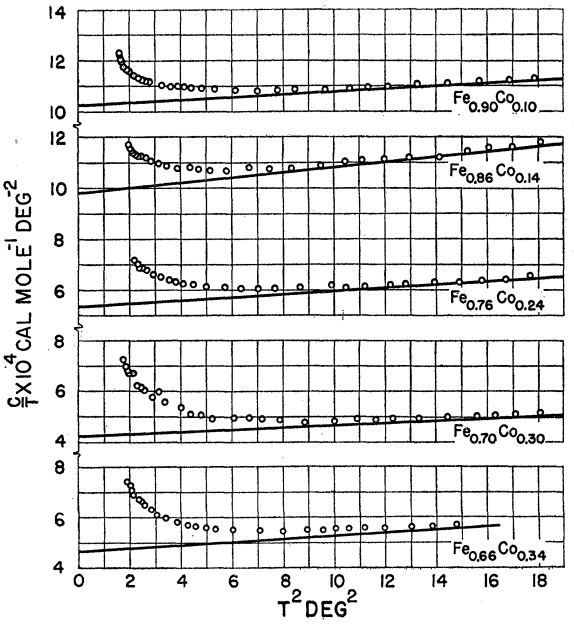

FIG. 10. Specific heat of bcc Fe-Co solid solutions. [Solid lines represent electronic plus lattice contribution, as calculated from Eq. (2).]

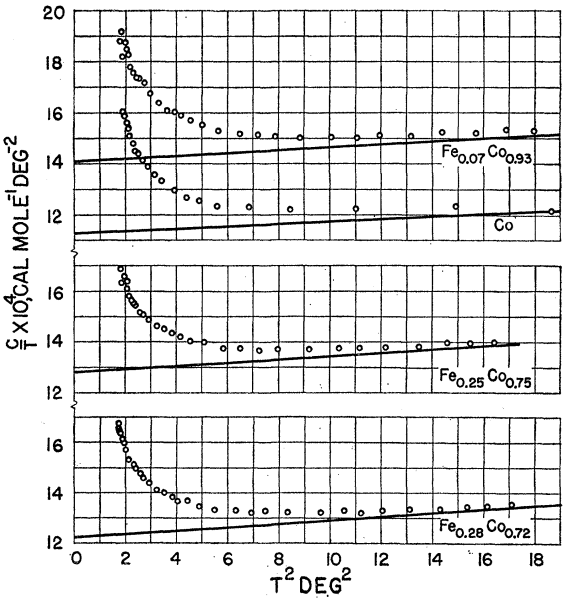

FIG. 12. Specific heat of Fe-Co solid solutions. [Solid lines represent electronic plus lattice contribution, as calculated from Eq. (2).]

TABLE III. Specific heat results. Estimated over-all accuracy of γ values is $\pm 2\%$, that of θ is $\pm 15°$K.

Alloy	Crystal Structure	$\gamma \times 10^4$ cal mole^{-1}deg^{-2}	β cal mole^{-1}deg^{-4}	α cal mole^{-1}deg	ϵ $\pm\%$	θ °K	H_{eff} k gauss
$Ti_{0.5}V_{0.5}$	bcc	~22					
$V_{0.77}Cr_{0.23}$	bcc	14.2	0.0410		0.3	484	
$V_{0.5}Cr_{0.5}$	bcc	11.6	0.1507		0.3	314	
$V_{0.26}Cr_{0.74}$	bcc	5.31	0.0663		0.4	412	
$V_{0.2}Cr_{0.8}$	bcc	5.15	0.0627		0.5	420	
$V_{0.1}Cr_{0.9}$	bcc	5.17	0.0373		0.3	500	
$V_{0.05}Cr_{0.95}$	bcc	5.54	0.0469		0.2	463	
$Cr_{0.9}Mn_{0.1}$	bcc	5.33	0.0454		0.4	467	
$Cr_{0.8}Mn_{0.2}$	bcc	<16	...				
$Cr_{0.69}Mn_{0.31}$	bcc	<29	...				
$Cr_{0.61}Mn_{0.39}$	bcc	<47	...				
$Cr_{0.5}Mn_{0.5}$	bcc	<56 (60.6)	(−0.249)		1.2		
$V_{0.92}Fe_{0.08}$	bcc	16.1	0.0666		0.2	412	
$V_{0.85}Fe_{0.15}$	bcc	12.4	0.0397		0.2	489	
$V_{0.8}Fe_{0.2}$	bcc	9.4	0.0352		0.6	509	
$V_{0.76}Fe_{0.24}$	bcc	~10.0	...				
$V_{0.74}Fe_{0.26}$	bcc	<13	...				
$V_{0.72}Fe_{0.28}$	bcc	<18.5	...				
$V_{0.7}Fe_{0.3}$	bcc	<21	...				
$V_{0.69}Fe_{0.31}$	bcc	<22 (22.9)	(−0.0516)		0.3		
$V_{0.66}Fe_{0.34}$	bcc	16.7	0.0867		0.4	377	
$V_{0.55}Fe_{0.45}$	bcc	13.1	0.0468		0.5	463	
$V_{0.33}Fe_{0.67}$	bcc	8.63	0.0917		0.4	369	
$Cr_{0.98}Fe_{0.02}$	bcc	<7.7	...				
$Cr_{0.95}Fe_{0.05}$	bcc	<16.6	...				
$Cr_{0.90}Fe_{0.10}$	bcc	25.2	0.353		0.4	236	
$Cr_{0.84}Fe_{0.16}$	bcc	32.2	0.355		0.5	235	
$Cr_{0.82}Fe_{0.18}$	bcc	39.4	0.0405		0.5	486	
$Cr_{0.81}Fe_{0.19}$	bcc	<41 (42.4) (43.0)[a]	(−0.086) (−0.123)[a]				
$Cr_{0.80}Fe_{0.20}$	bcc	37.3	0.0151		0.4	675	
$Cr_{0.70}Fe_{0.30}$	bcc	28.4	0.0433		0.5	475	
$Cr_{0.63}Fe_{0.37}$	bcc	16.4	0.171		0.4	301	
$Cr_{0.53}Fe_{0.47}$	bcc	14.3	0.137		0.4	324	
$Cr_{0.22}Fe_{0.78}$	bcc	9.87	0.0768		0.6	392	
$Cr_{0.15}Fe_{0.85}$	bcc	9.36	0.0632		0.4	419	
$Cr_{0.06}Fe_{0.94}$	bcc	10.2	0.0433		0.6	475	
Fe	bcc	11.9	0.0527		0.4	445	
$Fe_{0.90}Co_{0.10}$	bcc	10.3	0.0553	3.50	0.3	438	395
$Fe_{0.86}Co_{0.14}$	bcc	9.79	0.105	4.62	0.3	353	367
$Fe_{0.76}Co_{0.24}$	bcc	5.38	0.0593	5.40	0.3	428	308
$Fe_{0.70}Co_{0.30}$	bcc	4.24	0.0460	7.01	1.0	466	312
$Fe_{0.66}Co_{0.34}$	bcc	4.65	0.0648	6.88	0.2	415	292
$Fe_{0.62}Co_{0.38}$	bcc	4.06	0.0547	8.31	0.5	439	306
$Fe_{0.49}Co_{0.51}$	bcc	6.47	0.0764	10.7	0.4	393	297
$Fe_{0.40}Co_{0.60}$	bcc	8.94	0.0430	10.4	0.4	476	270
$Fe_{0.31}Co_{0.69}$	bcc	10.9	0.0946	15.5	1.0	366	309
$Fe_{0.28}Co_{0.72}$	bcc	12.2	0.0686	9.77	0.3	408	238
$Fe_{0.25}Co_{0.75}$	bcc	12.8	0.0636	9.17	0.5	418	227
$Fe_{0.07}Co_{0.93}$	fcc	14.11	0.0559	12.3	0.5	436	236
Co	hcp	11.3	0.0451	12.0	0.4	469	225

[a] Measured in magnetic field.

heating cycle. In later experiments this difficulty was avoided by first raising the temperature of the liquid helium bath from 1.2° to 1.5°K, and then lowering it again before starting the measurements, as described by Garfunkel and Wexler.[11] The other data in Fig. 3 show conditions obtainable when this precaution is observed. As seen in Fig. 4, the random errors for alloy $Cr_{0.5}Mn_{0.5}$ are larger than for the other Cr-Mn alloys, presumably largely due to the poor heat conductivity in this alloy. Because of the specific heat anomaly, observed for all these alloys except $Cr_{0.9}Mn_{0.1}$, the data could not be fitted to Eq. (1). As discussed more fully below, similar anomalies also occur in certain V-Fe alloys, Figs. 5 and 6, and in some Cr-Fe alloys, Figs. 7 and 8. In all these cases, the γ values listed in Table III are estimates based on the lowest C/T values

[11] M. P. Garfunkel and A. Wexler, Rev. Sci. Instr. **25**, 170 (1954).

obtained for each alloy. The Debye temperature could not be measured for any of these alloys. The specific heat determinations made in the presence of a magnetic field for alloy $Cr_{0.81}Fe_{0.19}$ (filled circles in Fig. 8) show much higher random errors than usual, because of the small mass of this specimen.

As seen in Figs. 10 to 12, in the Fe-Co system a specific heat anomaly occurs toward the lower end of the temperature range of the measurements. The extent of the anomaly increases with increasing Co content, but its presence is clearly established for all Fe-Co alloys, including the fcc one. The measured specific heat values could be expressed in the form

$$C=\gamma T+\beta T^3+\alpha T^{-2}, \qquad (2)$$

with a standard deviation of 0.2 to 1%, Table III. The third term here represents the contribution from hyperfine interaction between the dipole moment of Co^{59} nuclei with the effective field H_{eff} at the nucleus.[12] Calculation of H_{eff} from the coefficient α gives values increasing with increasing Fe concentration, as shown before by Arp, Edmonds, and Petersen,[13] but the numerical values (Table III) are somewhat higher than those reported by them. The H_{eff} values obtained by Arp *et al.* are undoubtedly more accurate than those given in Table III since, in the temperature range 0.35° to 0.7°K used by them, the anomaly is more prominent. Conversely, the temperature range of 1.4° to 4.2°K, used in the present work, gives more accurate results in determining γ than the lower temperature range used by Arp *et al.* It is probable that the rather high γ values reported by those investigators for Co and for $Fe_{0.40}Co_{0.60}$ are less accurate than the values given in Table III.

The specific heat anomaly, shown by several V-Fe, Cr-Fe, and Cr-Mn alloys (Figs. 4 to 9), occurs in relatively narrow composition ranges, namely at compositions corresponding in each system to the steep rise in γ with increasing Fe or Mn content, respectively (Figs. 13, 14). The temperature dependence of this anomaly is distinctly different from that of the anomaly discussed in the previous paragraph. For the anomaly now under discussion a separation of the specific heat into the three terms of Eq. (2) gives negative values for the constant β, and hence negative apparent Debye temperatures. Since this is impossible, it may be concluded that this type of anomaly can not be described by a term of the form αT^{-2}. The anomalous specific heat term here decreases more slowly with increasing temperature than would correspond to the T^{-2} relationship. It is quite possible that this anomaly is a result of relatively long-range interactions of the magnetic moments of Fe or Mn atoms dispersed in a nonmagnetic or weakly magnetic matrix. The anomaly observed by

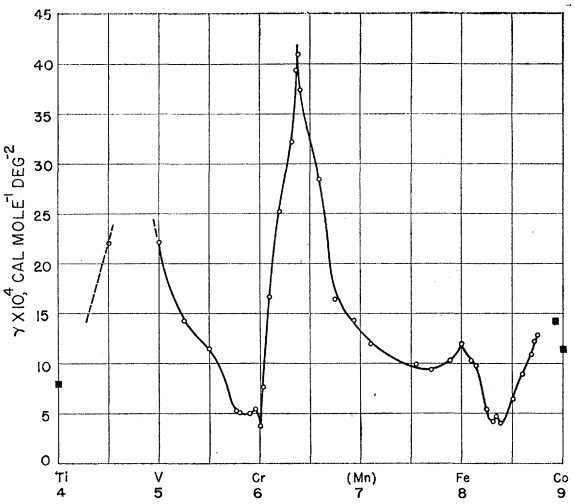

FIG. 13. γ vs electron concentration for Ti-V, V-Cr, Cr-Fe, and Fe-Co alloys. {γ values taken from earlier publications for Ti [N. M. Wolcott, Phil. Mag. **2**, 1246 (1957)], V [W. S. Corak, B. B. Goodman, C. B. Satterthwaite, and A. Wexler, Phys. Rev. **102**, 656 (1956)], Cr [I. Estermann, S. A. Friedberg, and J. E. Goldman, Phys. Rev. **87**, 582 (1952)], and $Cr_{0.45}Fe_{0.55}$.[16] Filled squares represent data for close-packed structures.}

Guthrie, Friedberg, and Goldman[14] in Cu-Ni alloys occurs at a composition corresponding to the beginning of ferromagnetism in that alloy system, and it shows a temperature dependence similar to that characteristic of the phenomenon just discussed. De Nobel and

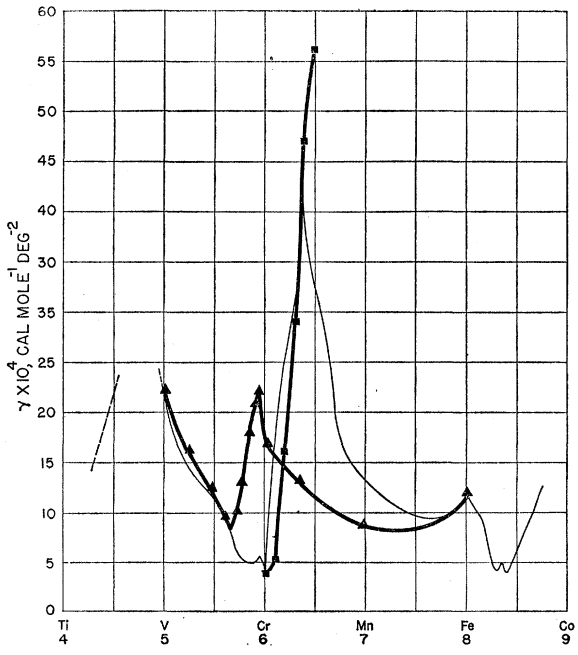

FIG. 14. γ vs electron concentration for bcc V-Fe solid solutions (filled triangles) and for bcc Cr-Mn solid solutions (solid squares). Thin line duplicates curve in Fig. 13 for comparison.

[12] W. Marshall, Phys. Rev. **110**, 1280 (1958).

[13] V. Arp, D. Edmonds and R. Petersen, Phys. Rev. Letters **3**, 212 (1959).

[14] G. L. Guthrie, S. A. Friedberg, and J. E. Goldman, Phys. Rev. **113**, 45 (1959).

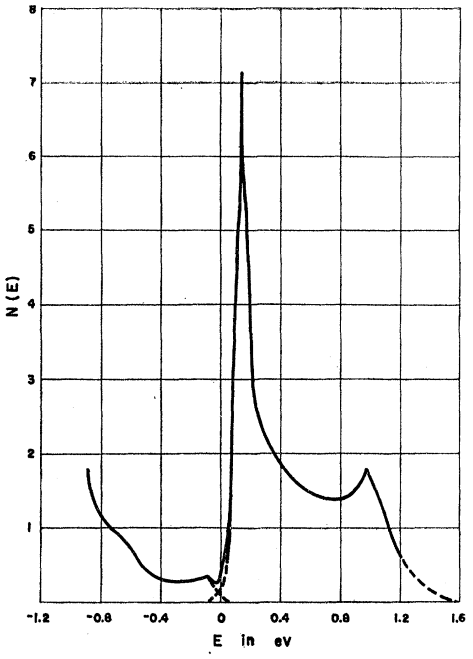

FIG. 15. $N(E)$, in number of states per atom per electron-volt, vs E, in electron-volts, for V-Cr, Cr-Fe, and Fe-Co alloys, calculated from data in Fig. 13.

Du Chatenier[15] recently found that the specific heat anomaly in dilute Ag-Mn and Cu-Mn alloys has a similar temperature dependence, and that this anomaly is reduced in magnitude when the specific heat measurements are carried out in a magnetic field.

The specific heat anomaly exhibited by the $V_{0.69}Fe_{0.31}$ alloy and the $Cr_{0.89}Fe_{0.19}$ alloy may be different in nature from both anomalies previously discussed. In these cases, and also for $Cr_{0.5}Mn_{0.5}$, the C/T vs T^2 graph has no pronounced curvature, but it has a negative slope in the whole temperature range (Figs. 4, 6, 8). At least in the case of $Cr_{0.89}Fe_{0.19}$ no decrease in the magnitude of the anomaly was found when the specific heat measurements were carried out in a magnetic field. It is true that the significance of this observation may be limited by the relatively low accuracy of the measurements carried out in the magnetic field, and also by the low intensity (1000 oe) of the magnetic field used. Nevertheless, the characteristic temperature dependence, as described above, appears to occur specifically in alloys of a composition very nearly corresponding to the maximum value of γ in both the V-Fe and Cr-Fe systems. Also, at least in the Cr-Fe system, the compositions showing the "magnetic-type" anomaly (2% and 5% Fe) are clearly separated from the composition (19% Fe) where the "peak-type" anomaly occurs; alloys $Cr_{0.9}Fe_{0.1}$, $Cr_{0.84}Fe_{0.16}$, and $Cr_{0.82}Fe_{0.18}$, of intermediate composition, show no anomalies. It is quite possible that this "peak-type" anomaly is associated with the sharp curvature of the $N(E)$ vs E curve at the maximum of γ (Fig. 15).

The estimated over-all accuracy of the γ values is $\pm 2\%$ for those cases where the C vs T data could be fitted to one of the two equations given above. The estimated accuracy of the θ values listed in Table III is $\pm 15°$K. In Figs. 10 to 12 the straight lines, which the data points approach near 4.2°K, have been plotted by using the γ and β values obtained for each alloy by least squares calculation from Eq. (2).

DISCUSSION

A notable feature of the data obtained for the Cr-Fe, Cr-Mn, and V-Fe systems is the high peak of γ at certain alloy compositions. Since previously measured electronic specific heat coefficients for bcc metals and alloys were much lower, the question arises whether or not the high γ values observed in the present work may be properly interpreted as electronic specific heat coefficients relating to the bcc alloy phase. Some alternative possibilities that might be considered are the following: (1) Transformation into a more complex crystal structure during cooling from room temperature to the temperature range of the specific heat measurements. Hoare and Matthews[16] found that $Cr_{0.45}Fe_{0.55}$, after transforming into the sigma phase, has a much higher γ value than it has in the bcc form. (2) A sizable contribution to the term of the specific heat linear in temperature, resulting from the ferromagnetic to paramagnetic transformation. The Curie temperature of alloys near the composition $Cr_{0.8}Fe_{0.2}$ may be expected to be quite low.[17] (3) Other specific heat contributions of magnetic origin, such as that due to spin waves, or the one recently considered by Marshall.[18]

Regarding the question of a possible phase transformation, only the diffusionless type needs to be considered, in view of the temperature range under consideration. It is not likely that a martensitic distortion of the lattice would entail a change in electronic structure sufficiently drastic to account for a very large increase in the density of states at the Fermi level, similar to that found for the complex (Fe, Cr)σ phase.[16] The formation of such a complex structure from the bcc one does involve diffusion. Measurement of the electrical resistivity of Cr-Fe alloys as a function of temperature[19] in fact indicated no phase transformation between 300° and 4.2°K. Particularly clear-cut are the results for the alloy $Cr_{0.8}Fe_{0.2}$, with a γ value near the maximum; the resistivity anomaly observed in alloys lower in Fe, which is apparently due to the antiferromagnetic transition, is in this alloy completely absent.

In assessing the possibility of an important contribu-

[15] J. De Nobel and F. J. Du Chatenier, Physica **25**, 969 (1959).

[16] F. E. Hoare and J. C. Matthews, Proc. Phys. Soc. (London) **71**, 220 (1958).

[17] A. Arrott (private communication).

[18] W. Marshall (to be published).

[19] N. S. Rajan, R. M. Waterstrat, and Paul A. Beck, J. Appl. Phys. **31**, 731 (1960).

tion to γ at 1.4° to 4.2°K from the magnetic specific heat, knowledge of the magnetic transition temperature is essential. Nevitt[20] measured the magnetization at various temperatures for some of the same alloy specimens previously used for the low-temperature specific heat measurements here reported. He found a Curie temperature of 50°±5°K for the $Cr_{0.82}Fe_{0.18}$ alloy and 70°±5°K for the $Cr_{0.81}Fe_{0.19}$ alloy, assuming that Arrott's criterion[21] is applicable in these cases. These values are consistent with the Curie temperature for alloys with higher Fe contents.[22] In the case of the V-Fe alloys, extrapolation of the Curie temperatures and saturation moments obtained by earlier workers for the Fe-rich alloys, and those obtained by Nevitt[23] for $V_{0.47}Fe_{0.53}$ and for $V_{0.40}Fe_{0.60}$, suggests that ferromagnetism could appear only in alloys with 35% Fe or more. Consequently, in this system, alloys at the maximum of γ are almost certainly not ferromagnetic even at liquid He temperatures. The bcc Cr-Mn solid solutions are antiferromagnetic, with the Néel temperature increasing from 308°K at 0% Mn[24] to approximately 463°K at 1% Mn,[25] to well above 573°K at 50% Mn.[26] The contribution of the magnetic specific heat to the γ values measured below 4.2°K for the Cr-Mn alloys should be negligibly small. For the Cr-Fe alloys with 18% and 19% Fe, the Curie temperature is 12 to 50 times higher than the temperatures at which the specific heat measurements were carried out so that, even here, the magnetic specific heat contribution would be far too small to account for the observed high γ values. Recent measurements by Schröder[27] of the specific heat at room temperature of bcc Cr-Fe alloys showed that, in addition to the maximum of the specific heat vs composition curve at approximately 35% Fe resulting from the magnetic transformation at room temperature, there is also a second, well-separated maximum at 19% Fe. Since this second maximum is at the same composition where the γ peak is located at liquid He temperatures, and since its magnitude is accounted for quite well on the assumption that the value of γ up to room temperature is the same as the value measured below 4.2°K, Schröder's results show that the maximum of γ at $Cr_{0.81}Fe_{0.19}$ cannot be the result of any of the magnetic effects considered.

Several of the C/T vs T^2 curves (Figs. 4, 5, 7, 8) show considerable anomalies, particularly at the low side of the temperature range of measurements. These anomalies have been discussed in some detail in a previous section. It should be pointed out here that the anomalies are evidently not responsible for the high γ values observed. This is particularly clearly shown by the $Cr_{0.80}Fe_{0.20}$ alloy, which has a γ value near the maximum, but shows no anomaly. Similarly, $Cr_{0.84}Fe_{0.16}$ and $Cr_{0.82}Fe_{0.18}$ have quite high γ values, without anomalies.

All experimental results discussed are consistent with the interpretation of γ as the electronic specific heat coefficient. This interpretation is further strengthened by the observation that the peak values of γ in the three systems Cr-Fe, Cr-Mn, and V-Fe occur at compositions corresponding at least roughly to the same electron concentrations (average number of electrons per atom outside the argon shell), Figs. 13 and 14. It may be, therefore, assumed that the γ values listed in Table III, from which contributions due to anomalies have been separated as well as possible, are representative of the density of states at the Fermi surface in the various alloys.

The question as to the consistency of the very high density-of-states values observed at certain alloy compositions with theoretical calculations may be considered briefly. Figure 15 shows the density of d states vs Fermi energy, derived from the measured γ vs electron concentration curve given in Fig. 13, following the method described by Hoare, Matthews, and Walling.[28] In the derivation all measured γ values were decreased by 1.7×10^{-4} cal mole^{-1}deg^{-2} (the γ value for Cu) on the assumption that, in first approximation, this value represents the contribution of the s band to the electronic specific heat coefficient. The correlation $\gamma=\frac{2}{3}\pi^2k^2N(E)$ was used for calculating $N(E)$ for the nonmagnetic V-Cr alloys. For the other parts of the curve, corresponding to magnetic alloys, the relationship $\gamma=\frac{1}{3}\pi^2k^2N(E)$ was used. In the Fermi energy scale $E=0$ was set at the point corresponding to Cr, in accordance with the convention adopted in a recent paper by Belding.[29] The density of states vs Fermi energy curve derived from the present results, Fig. 15, bears close resemblance to the corresponding curve calculated by Belding (see figure in reference 29), on a tight-binding model, taking into account second-nearest neighbor interactions as well as nearest ones. Consequently, the density-of-states interpretation of the measured γ values does not appear to be inconsistent with theory.

Figure 13 shows the γ values vs the electron concentration for the systems Ti-V, V-Cr, Cr-Fe, and Fe-Co. Very low values of γ are found near Cr and near $Fe_{0.65}Co_{0.35}$, and these separate from each other three regions of electron concentration with high γ values, corresponding to high density of states at the Fermi level. The first region of high density of states is at alloy compositions where the atomic magnetic moments are zero. The second region of high density of states corresponds to alloys which have increasing magnetic moment with increasing electron concentra-

[20] M. V. Nevitt (private communication).
[21] A. Arrott, Phys. Rev. **108**, 1394 (1957).
[22] F. Adcock, J. Iron Steel Inst. (London) **124**, 99 (1931).
[23] M. V. Nevitt (private communication).
[24] L. M. Corliss, J. M. Hastings, and R. J. Weiss, Phys. Rev. Letters **3**, 211 (1959).
[25] G. deVries, J. phys. radium **20**, 438 (1959).
[26] J. S. Kasper and R. M. Waterstrat, Phys. Rev. **109**, 1551 (1958).
[27] K. Schröder, Phys. Rev. **117**, 1500 (1960).
[28] F. E. Hoare, J. C. Matthews, and J. C. Walling, Proc. Roy. Soc. (London) **A216**, 502 (1953).
[29] E. F. Belding, Phil. Mag. 4, 1145 (1959).

tion. In this region the Slater-Pauling curve rises from a point near Cr up to the composition $Fe_{0.65}Co_{0.35}$.[30,31] The third region of high density of states was found to start near $Fe_{0.65}Co_{0.35}$ and to extend to the limit of the bcc solid solutions at $Fe_{0.25}Co_{0.75}$. In this third region the Slater-Pauling curve shows decreasing magnetic moments with increasing electron concentration. These findings may be tentatively described in a simple manner in terms of three sub-bands, which appear to overlap only slightly and which, together, constitute the *d* band for these bcc alloys. The first sub-band apparently contains paired electrons, with no unopposed spin. If preliminary diffraction results[32] for Cr are confirmed, the number of localized *d* electrons contributing to the coherent scattering of x rays by Cr may be quite small. It is quite possible that the *d* electrons in the first sub-band (i.e., up to Cr), which presumably give rise to the high density of states at the Fermi level near V, may be described by wave functions showing relatively little tendency to be "localized" at the atoms. This would be consistent with Pauling's interpretation of the role of the *d* electrons (up to Cr) in bonding ("bonding orbitals").[31] The electrons in the second sub-band are apparently arranged with their spins aligned parallel. A tendency for localization at the atoms of the wave functions corresponding to these *d* electrons with unpaired spins is clearly indicated by Shull and Wilkinson's results with magnetic scattering of neutrons.[33] Clearly, in regard to the electrons of the second sub-band the observations cited are at least qualitatively consistent with Pauling's picture of "atomic orbitals."[31] Also, the calculations of Wood[34] for Fe, which suggest that near the top of the *d* band the wave functions may be considerably more localized than near the bottom, appear to be entirely consistent with the above interpretation of the experimental results. In the third sub-band, which can be built up within the composition range of the bcc structure (in Fe-Co alloys) only to a limited extent, the electrons must be assumed to have their spins aligned antiparallel with respect to the spins of the electrons in the second sub-band, in order to account for the known saturation magnetization values for these alloys, as shown in the Slater-Pauling curve.[30,31] It may be expected that the *d* electrons in the third sub-band also tend to be localized.

By analogy with the Cr-Fe system, it may be expected that in the bcc V-Fe solid solutions as well the sharp rise in γ with the electron concentration, following the γ minimum at $V_{0.78}Fe_{0.22}$ (Fig. 14), represents the beginning of the second sub-band, that is the appearance of magnetic moments associated with the Fe atoms in the alloy. Although ferromagnetism probably does not occur in this system at Fe contents less than about 35 at. %, if the above interpretation of the *3d*-band structure is correct, the presence of unaligned atomic moments in the composition range 25–35 at. % Fe should be detectable by means of magnetic susceptibility measurements. The presence of atomic moments and the weakness of the forces that tend to align them is quite likely to be responsible for the low-temperature specific heat anomaly observed below 4°K in this composition range (Fig. 5).

It should be noted that the electronic specific heat results do not necessarily imply a rigid band model. The absence of a completely quantitative coincidence between the corresponding sections of the γ vs electron concentration curves for the V-Fe, Cr-Fe, and Cr-Mn systems (Fig. 14) may be of significance in this respect. It may be noted that in these three systems the peak value of γ becomes lower and the peak shifts toward lower electron concentrations with increasing separation from each other of the components in the first long period of the periodic table.

ACKNOWLEDGMENTS

We wish to express our appreciation for very helpful discussions with Professor F. Seitz, Professor J. Bardeen, Professor J. S. Koehler, Professor D. E. Mapother, and Professor R. M. Thomson and with Dr. W. Marshall, Dr. A. Arrott, and Dr. K. Schröder. We are indebted to Dr. M. V. Nevitt for making available to us his magnetization data for Cr-Fe and V-Fe alloys prior to publication. Special thanks are due to Dr. R. J. Weiss, who manifested his interest in this work by giving us generously of his time and of his valuable advice over a period of about two years.

[30] J. C. Slater, J. Appl. Phys. **8**, 385 (1937).
[31] L. Pauling, Phys. Rev. **54**, 899 (1938).
[32] R. J. Weiss and J. J. DeMarco, Revs. Modern Phys. **30**, 59 (1958).
[33] C. G. Shull and M. K. Wilkinson, Revs. Modern Phys. **25**, 100 (1953); and Phys. Rev. **97**, 304 (1955).
[34] J. H. Wood, Quarterly Progress Reports, Solid-State and Molecular Theory Group, Massachusetts Institute of Technology, April 15, 1958; October 15, 1958; January 15, 1959; July 15, 1959; and October 15, 1959 (unpublished).